Agenzia nazionale per le nuove tecnologie,
l'energia e lo sviluppo economico sostenibile

MINISTERO DELLO SVILUPPO ECONOMICO

Ricerca di Sistema elettrico

Studio sull'analisi termoidraulica di un sistema magnetico superconduttore per FAST

F. Crisanti, G. Ramogida, G. M. Polli

Report RdS/PAR2014/061

STUDIO SULL'ANALISI TERMOIDRAULICA DI UN SISTEMA MAGNETICO SUPERCONDUTTORE PER FAST

F. Crisanti (ENEA), G. Ramogida (ENEA), G. M. Polli (ENEA)

Settembre 2015

Report Ricerca di Sistema Elettrico
Accordo di Programma Ministero dello Sviluppo Economico - ENEA
Piano Annuale di Realizzazione 2014
Area: Produzione di Energia Elettrica e Protezione dell'Ambiente
Progetto: B.3.2 Attività di fisica della Fusione complementari a ITER
Obiettivo: C2
Responsabile del Progetto: Ing. Aldo Pizzuto, ENEA

Indice

Sommario

Uno degli obiettivi principali della macchina JT-60SA è lo sviluppo di regimi di plasma a confinamento avanzato, necessari per poter dimostrare l'effettiva possibilità di realizzazione di un reattore a fusione "steady state" ovvero capace di rimanere in funzione per un tempo sufficientemente lungo da poter essere considerato stazionario non solo dal punto di vista della fisica dei plasmi ma anche da quello delle tecnologie. A tale scopo è di basilare importanza verificare la possibilità di utilizzare FAST per lo studio delle soluzioni, sia dal punto di vista dei componenti che da quello degli scenari, capaci di garantire lo smaltimento del flusso termico di un plasma quasi ignito in queste condizioni di regime "steady state".
Il sistema magnetico previsto nel progetto attuale di FAST prevede che tutte le bobine (di campo toroidale, esterne di campo poloidale e del solenoide centrale) siano realizzate in rame, con conseguente intrinseca limitazione della durata della scarica. Per realizzare invece una macchina capace di raggiungere regimi "steady state" sarà necessario fornire adeguati sistemi di Current Drive per la corrente di plasma, già previsti in FAST, e realizzare il sistema magnetico con bobine superconduttrici, analogamente a JT-60SA.
Uno dei problemi più critici di un sistema magnetico superconduttore è il suo comportamento dal punto di vista termico durante il funzionamento in condizioni operative e durante eventi anomali ed il relativo dimensionamento dei circuiti di raffreddamento al fine di garantire l'operatività del sistema e da evitare il suo danneggiamento in caso di guasto. E' stato perciò simulato e studiato in dettaglio l'andamento termico nel magnete toroidale durante le condizioni più critiche, considerando una bobina realizzata utilizzando lo spazio disponibile nel design attuale basato su conduttori in rame. E' stato quindi calcolato il margine minimo di temperatura nelle bobine considerando il carico termico sull'avvolgimento e sul jacket del cavo prodotto dal massimo carico neutronico previsto, incluso quello dovuto alla reazione secondaria D-T.

A tale scopo sono state effettuate le seguenti attività:

- Analisi elettro-termo-idraulica della soluzione concettuale per il magnete di campo toroidale, considerando il carico neutronico primario e secondario ed il massimo campo magnetico;
- Valutazione della necessità di uno schermo neutronico per il magnete.

1 Introduction

FAST (Fusion Advanced Studies Torus) is the Italian proposal for a new European satellite tokamak reactor aimed at supporting ITER activities and anticipating some DEMO relevant physics and technology issues [1,2]. It has been conceived as a compact (R_0 = 1.82 m) machine working at high field (B_T up to 8.5 T) and high plasma current (I_p up to 8 MA). Currently, FAST magnetic system is designed with 18 TF (Toroidal Field), 6 CS (Central Solenoid) and 6 PF (Poloidal Field) resistive coils, cooled by helium gas flow at 30 K. A feasibility study to verify whether a superconductive (SC) solution for the whole magnetic system would be possible or not, avoiding any major modifications to the machine geometry or scenarios, was studied at ENEA. In this frame the thermo-hydraulic analysis of the TF superconducting cable was carried out to verify the feasibility of the new SC design. Indeed, one of the main critical aspects in the operation of a superconducting TF magnet is the conductor heating due to both a direct energy deposition by neutrons and by secondary gamma generated during plasma operation. The operating temperature and the relevant temperature margin (i.e. the operating safety margin) of the magnet depend strongly on the heat loads and on the capability of the coolant to remove it. Starting from the reference layout proposed in [3], based on the 7.5 T H-mode reference scenario of FAST [1,2], some analysis were performed aimed at verifying the validity of the assumptions based, where possible, on the design parameters of similar machines [4]. Finally, the need for a neutron shield has been preliminarily assessed by comparing the effect of different nuclear heating thermal loads on the performance of the SC cable.

2 Activities description and results

2.1 Design of the Super Conducting Toroidal Field coils

The Super Conducting (SC) coils feasibility study presented in [3] and used in the present analysis has been centered on one of the most challenging scenarios among those foreseen during FAST activities, the H-mode reference scenario (B_T = 7.5 T, I_p = 6.5 MA), whose main engineering parameters are reported in [1] or [5]. It is worth noting that this scenario is characterized by a relatively short duration, in fact the flat top lasts 13 s.

Based on the room available in the resistive design, the SC version of the TF coil has been conceived. It consists of an approximately trapezoidal winding pack (WP), inserted into a stainless steel (SS) casing, wound from a rectangular conductor with an aspect ratio lower than 2, having long twist pitch values, low void fraction and no central channel. These choices, mainly aimed at giving better load support to the Nb_3Sn strands and consequent limited performance degradation, derive by many measurement campaigns and studies performed in the last years. Note that the choice of Nb_3Sn for the SC strand is required by the maximum magnetic field (around 14 T) arising in the coil. The main TF coil data are summarized in Table I.

Table I. TF conductor and WP main features

Inner dim. (mm^2)	13×21
Jacket thickness (mm)	2.8
Corner radius	2.5
# Strands (all SC)	360
Strand diam. (mm)	0.81
Cabling pattern	$3 \times 3 \times 5 \times 5 \times 6$
VF (%)	28.5
I_p (kA)	41.2
# Layer	10
# DP	3 central + 2 side
Central DP length	180 m
Side DP length	144 m

An artistic representation of the TF coil is shown in Fig. 1, where the stainless steel casing is represented using a transparent color to enable the view of the inner WP. In this regard, note that the SS casing external dimensions exactly coincide with those foreseen in the resistive design. Nonetheless, a preliminary stress analysis carried out on the present design has confirmed the reliability of the steel casing in withstanding the electromagnetic loads released during the magnet operations [3].

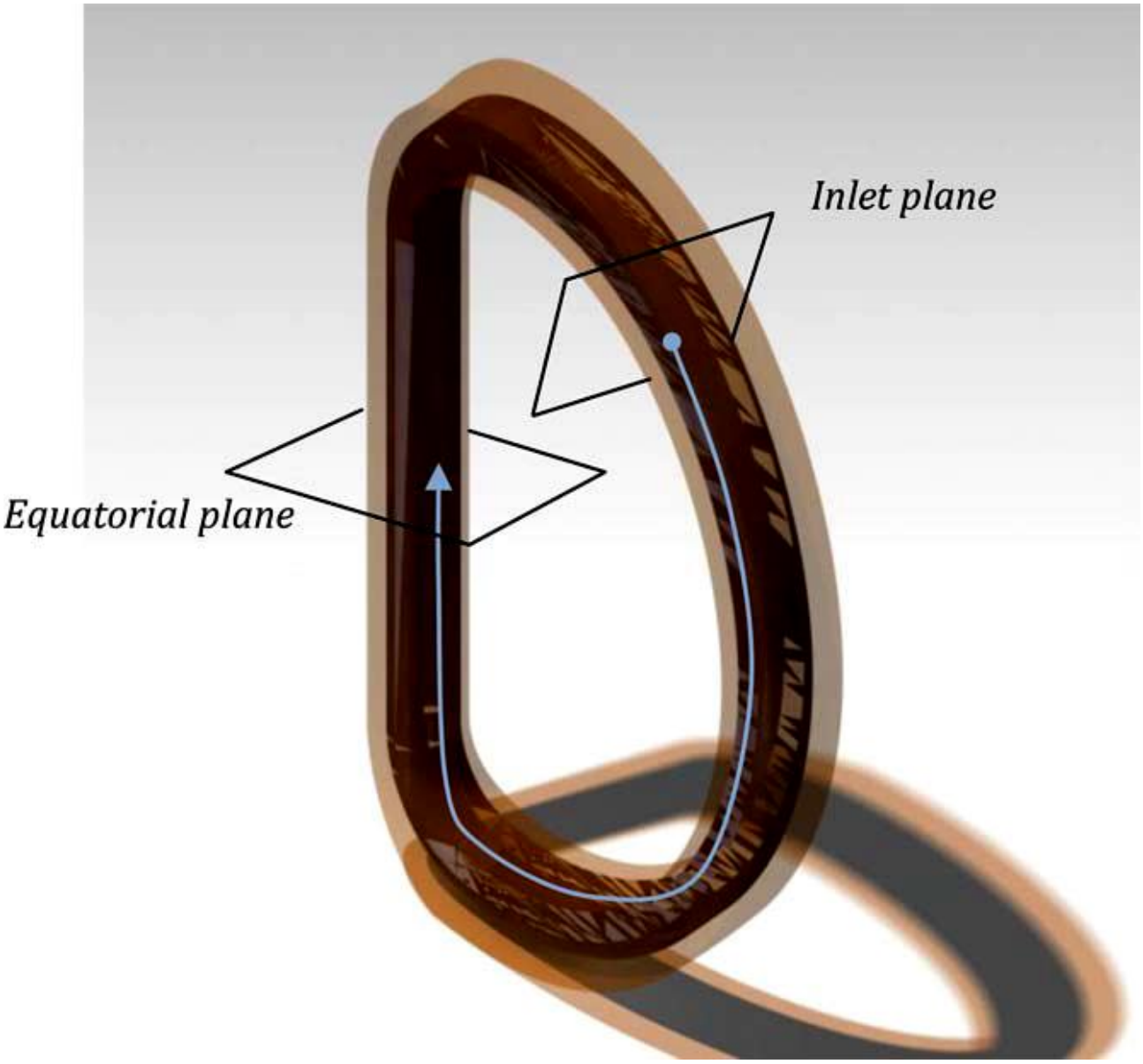

Figure 1. Artistic view of the SC TF coil, with the steel casing in transparent to show the internal SC WP

2.2 Nuclear Heating

The nuclear heating (NH) contribution to the operative temperature definition has been determined using data provided by a MCNP5 code 3-D analysis [6], ad-hoc performed for the superconducting magnets. In particular, it has been addressed to investigate if the introduction of a nuclear shield, which is obviously absent in the resistive design, would be necessary or avoidable.

In Fig. 2 the nuclear heating density is shown as function of an arbitrary radial position in the most irradiated zone, i.e. in the equatorial plane. The values refer to 1.2×10^{17} n/s (neutron rate corresponding to H-mode reference scenario) [6]. The nuclear heating arising in the resistive case is compared to the superconducting solution assuming different configurations. A homogeneous weighted mixture of Nb_3Sn,

Cu, He, stainless steel and epoxy resin, placed behind 2.5mm of SS casing with respect to plasma is used to simulate the winding pack and the casing. Three different design options for the superconducting solution are investigated: first a configuration without additional shield has been considered, then a 50mm thick shield, made by 80% SS and 20% water located behind the vacuum vessel has been inserted and finally, a more efficient type of shield, similar to that adopted for the ITER vacuum vessel with borated steel has been examined instead. Note that a 20% reduction in nuclear heating in the first conductor layer of the coil in the equatorial plane, with respect to the first SC solution, would be reached using the first shield and almost a 50% reduction would be possible in the more efficient (but also more expensive) ITER-like option.

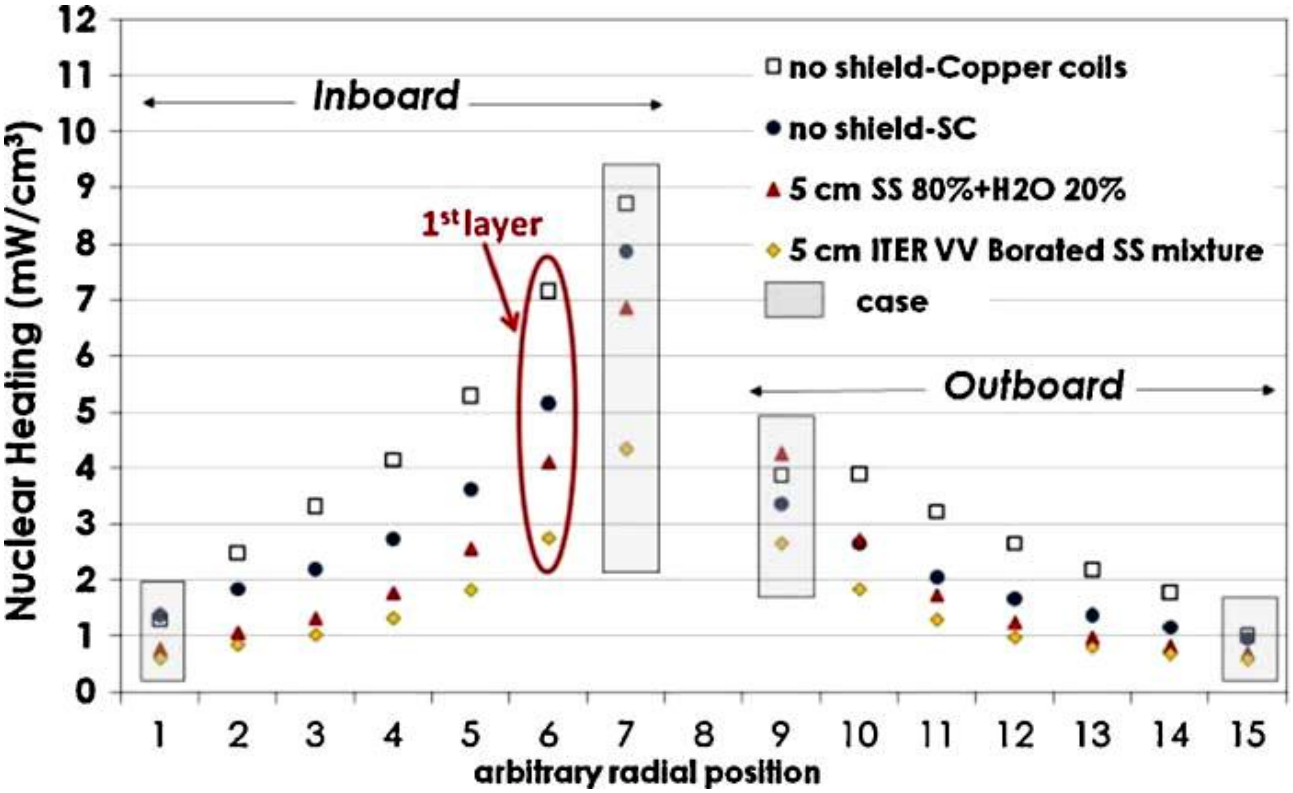

Figure 2. TF coil NH radial profile showing the effect of the presence of a nuclear shield

The distribution along the cable in the most critical pancake (see Fig. 1) has been obtained by scaling the data computed in other planes in [6]. In this regard, assuming that the helium inlet be at the pancake transition located in the outer leg facing the plasma, as suggested by Fig. 1, the thermo-hydraulic analysis has been carried out with respect to the most critical pancake that is the central one with the longest distance from inlet to equatorial plane [7]. Also, the radial distribution computed in the equatorial plane has been maintained in the other sections by a proper scaling. The result of this scaling is shown in Fig. 3. The two lines in the figure represent the thermal load applied to the strand bundle and to the steel conduit: these data have been used as input in the subsequent 1D electro-thermo-hydraulic analysis of the most critical pancake, at the end of burning (EOB). The two contributions have been maintained separate to emphasize the role of the active case cooling shown in the results. Note also that, whilst the heat deposited in the strand bundle has a strong effect on the stability of the conductor, the heat on the steel conduit affects only marginally the stability due to the short duration of the burning.

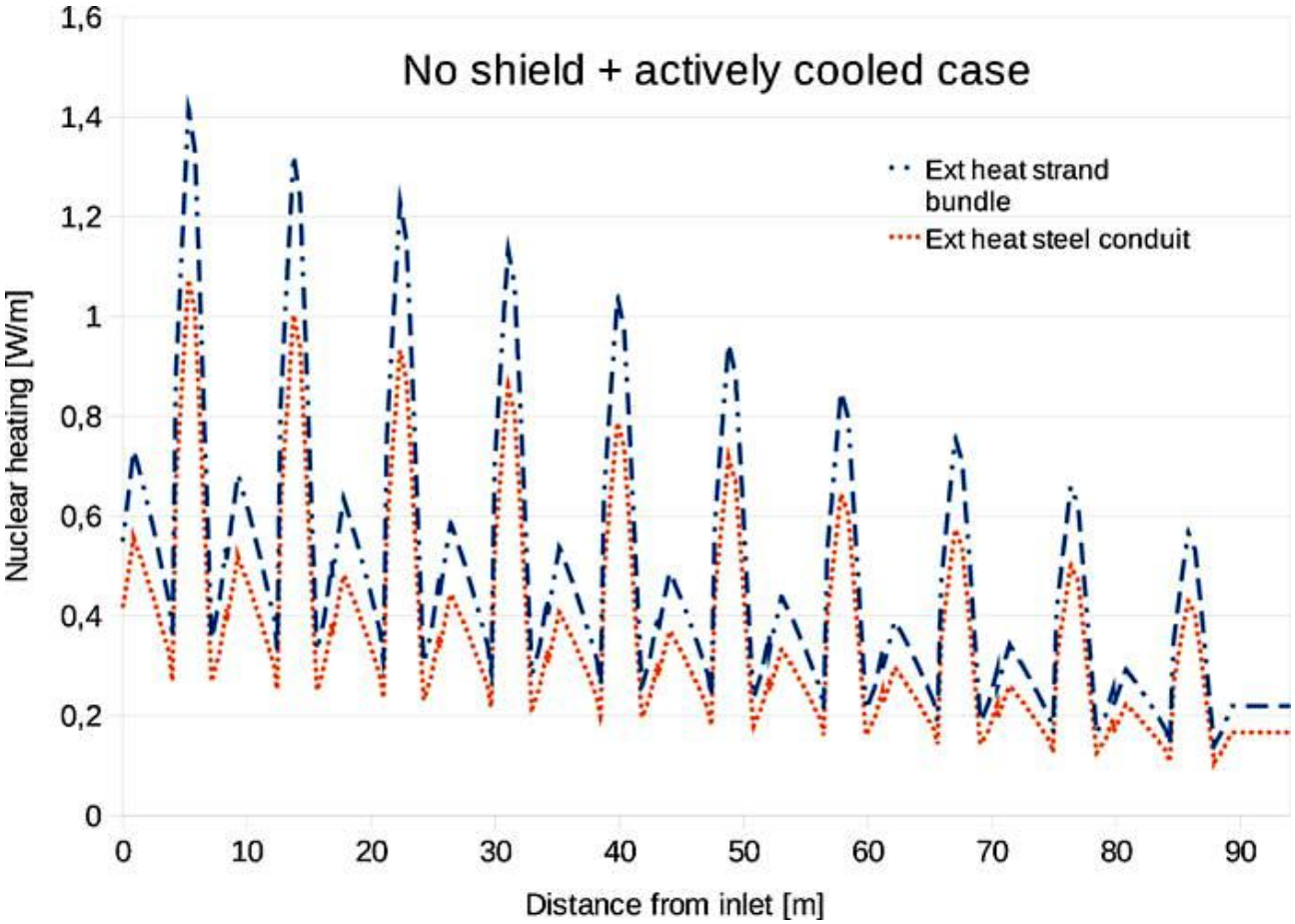

Figure 3. Nuclear heating distribution along the most critical pancake (the dotted line represents the contribution to the strand bundle, whereas the dot-dashed line reports the contribution belonging to the steel conduit)

On the other hand the nuclear heating evolution in time has been applied, according to Fig. 4 and Fig. 5. Indeed, two different scenarios have been conceived in the subsequent 1D electro-thermo-hydraulic analysis. In one case, the steel casing has been considered actively cooled by a set of channels capable to remove the heat generated in the casing due to neutrons (see Fig. 2); in the other case, the effect of heating from casing to WP has been retained into the model. Note that a 2D thermal transient analysis should be carried out in order to quantify the effect of the heat transfer from casing to WP and also its time evolution (see for instance [4] or [7]). However, since in the present design the steel casing geometry has not yet been defined, an estimate of the ratio of heat due to casing with respect to heat due to neutrons, and also of the time constant in the exponential decay after the EOB, have been made on the base of the results available in similar analysis [4].

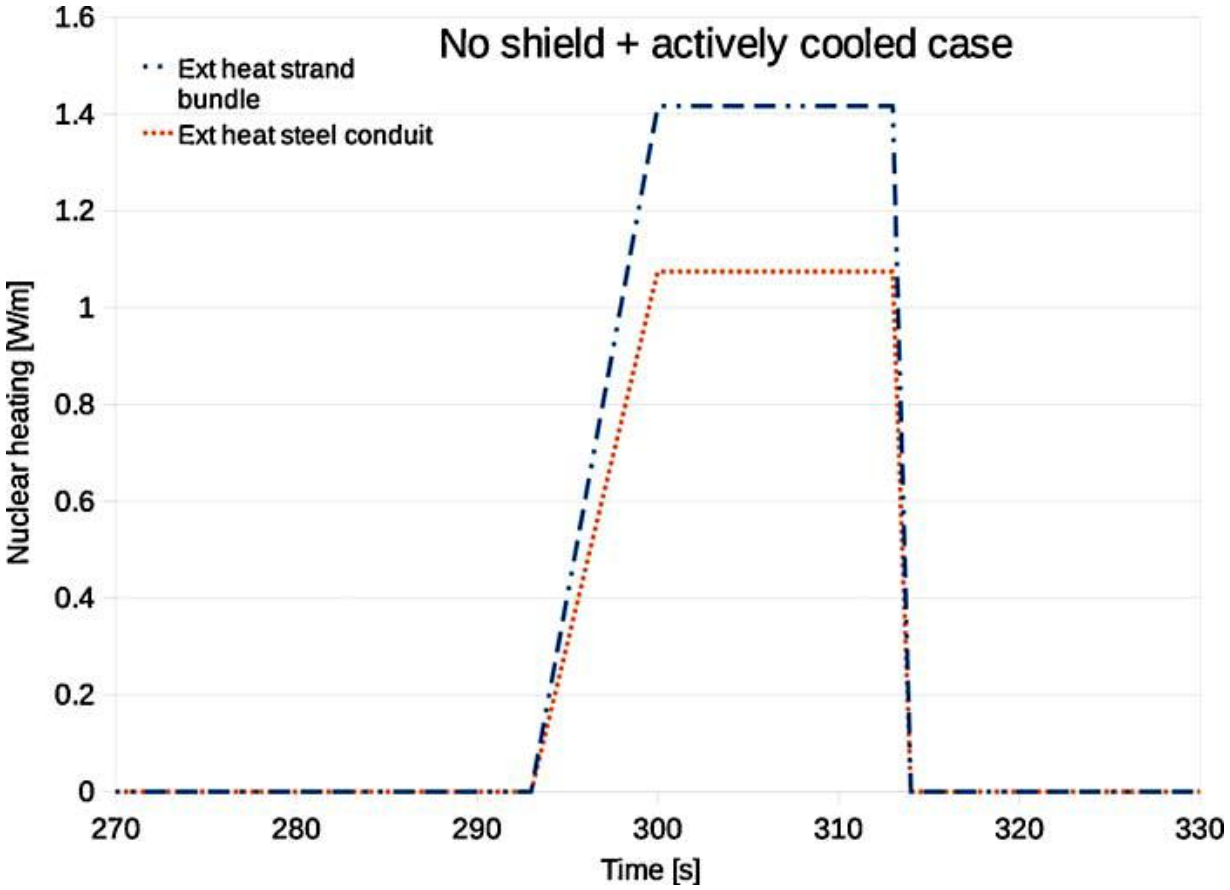

Figure 4. Time evolution of the nuclear heating when the steel casing is actively cooled

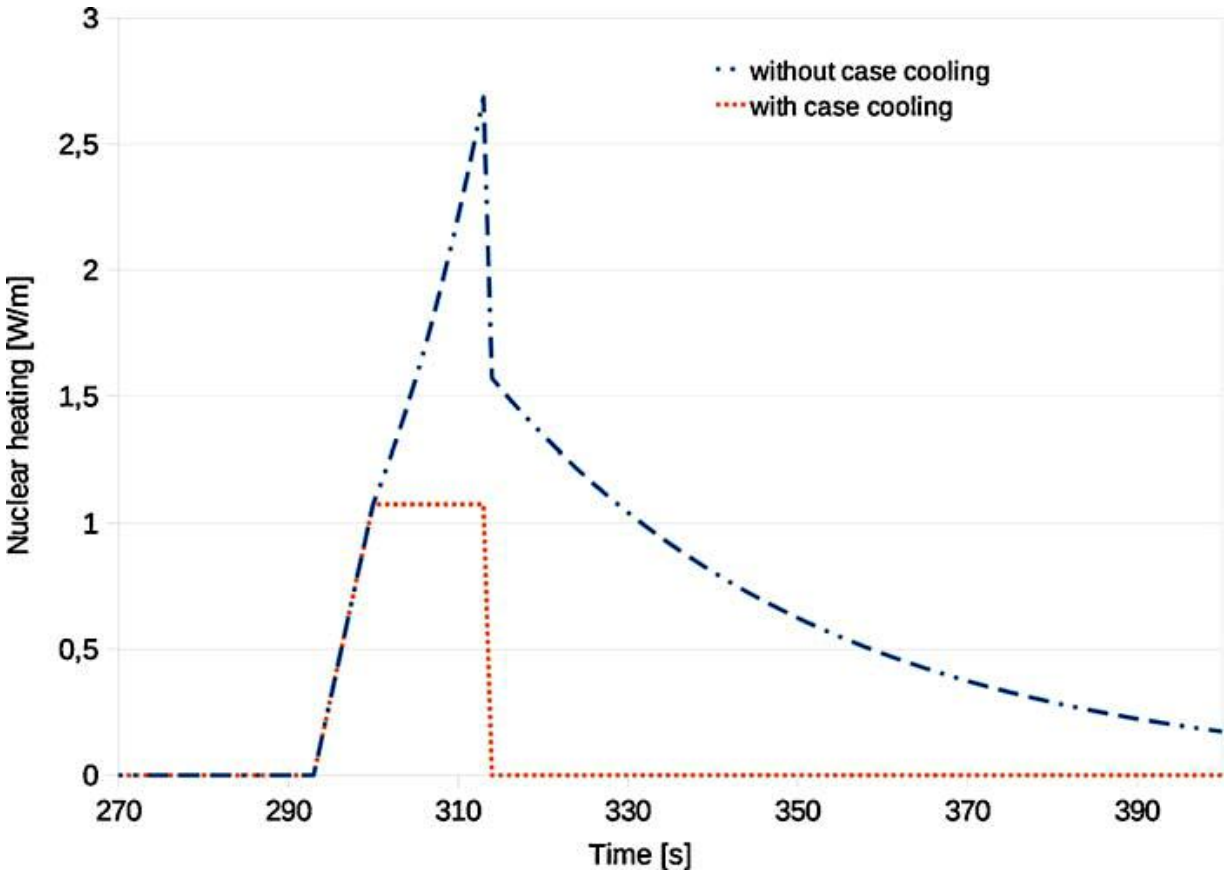

Figure 5. Time evolution of the nuclear heating in the steel conduit with and without steel casing cooling

Finally consider that the total power deposited at the central Double Pancake (DP) at the EOB in the different scenarios can be deduced from plots in Fig. 3 by integration over space and is reported in Table II. Note that part of the power reported in this table will be ejected away by convection by the flowing helium and part will be absorbed by the thermal capacity of the steel and the conductor.

Table II. Power [W] deposited at the EOB in the central Double Pancake (DP)

	Shield	No shield
Case cooling	117.6	157.5
No case cooling	193.7	259.4

2.3 Magnetic field

Another fundamental ingredient of the present analysis is the peak magnetic field intensity on the conductor cross section. Based on the field map in the first layer of the WP, computed from a complete 3-D electro-magnetic analysis of the whole scenario, a linear radial decay to zero has been assumed in the following layers. The field map has been considered constant in time throughout the simulation, maintaining for the whole scenario the worst magnetic conditions.
The maximum peak field B_{peak} = 14 T is found close to the equatorial plane, at 6 m from the helium inlet, where also the maximum nuclear heat is produced in the cable (see Fig. 3).

2.4 Results

The electro-thermo-hydraulic analysis has been carried out using the 1D code Gandalf [8]. Table III reports the nominal flow and strand conditions assumed in the reference layout. Moreover, in the reference layout the steel casing has been considered actively refrigerated (see Fig. 4) via a proper system of helium cooling channels. With these assumptions, the minimum temperature margin (defined as the difference between the “current-sharing” and the effective temperature of the conductor) is 0.98 K.

Table III. Reference flow and strand conditions

Property	Value
Mass flow rate	4 g/s
Helium inlet temperature	4.4 K
Helium inlet pressure	6 bar
Strand type	Nb3Sn “dipole” [9]
Applied strain	−0.46%

Fig. 6 shows the temperature margin distribution along the central pancake. Note that the minimum is at 6.4 m from the inlet immediately after the location where both nuclear heating and magnetic field reach their maxima and that the margin follows closely the magnetic field distribution along the cable. Note also that the computed pressure decay is ~3.13 bar, a not negligible value due to the low cable void fraction.
To quantify the effect of case cooling and neutron shield on the central pancake temperature margin, in Fig. 7 the minimum temperature margins are plotted in four different scenarios at the EOB and 7 s later. The four scenarios are:

(1) case cooling and no shield;
(2) case heating and no shield;
(3) case cooling and shield (80% steel and 20% water);

(4) case heating and shield (80% steel and 20% water).

It is apparent that the most critical one is that with no cooling and no shield (~0.8 K), conversely, the most stable one is that with case cooling and shield (~1.1 K).

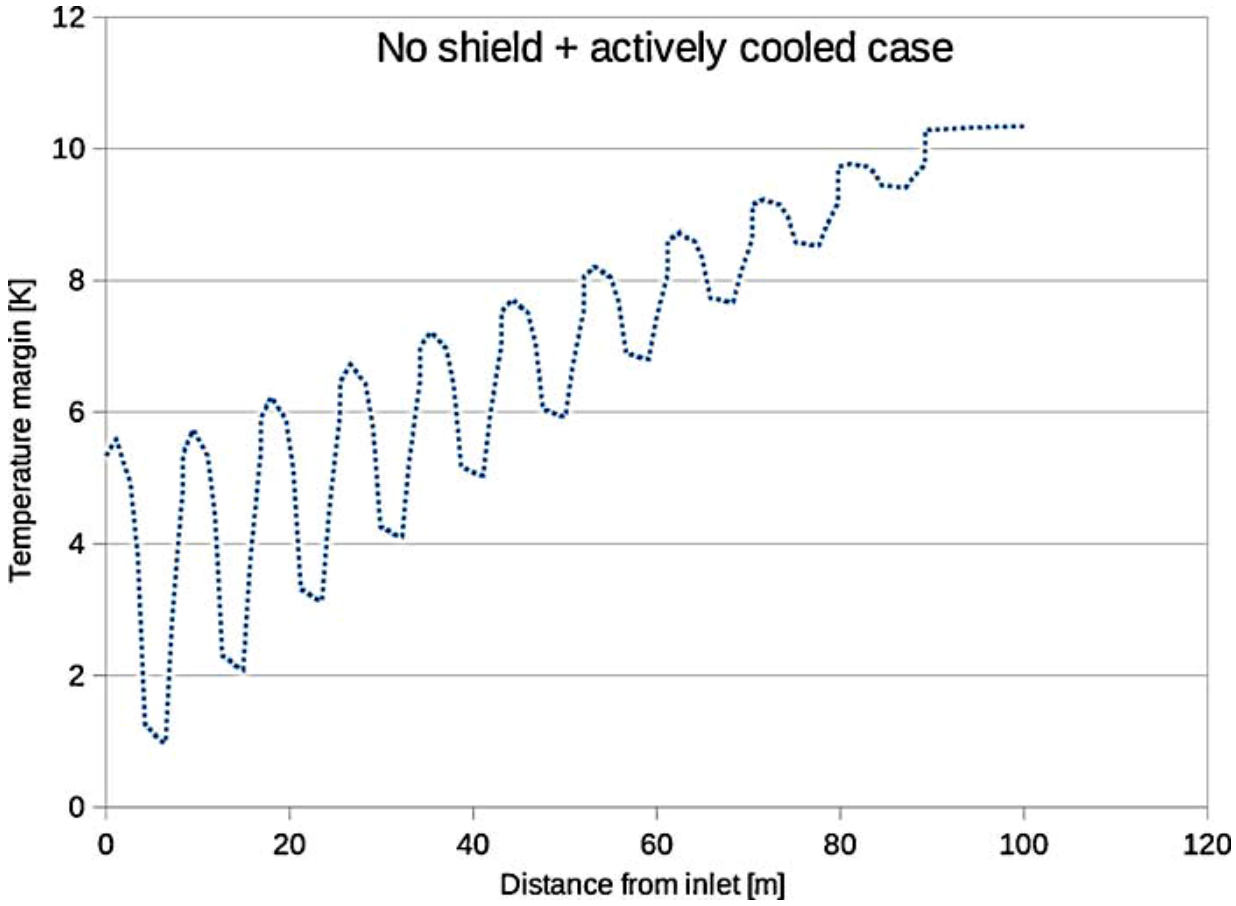

Figure 6. Temperature margin distribution along the central pancake in the case with case cooling and no shield

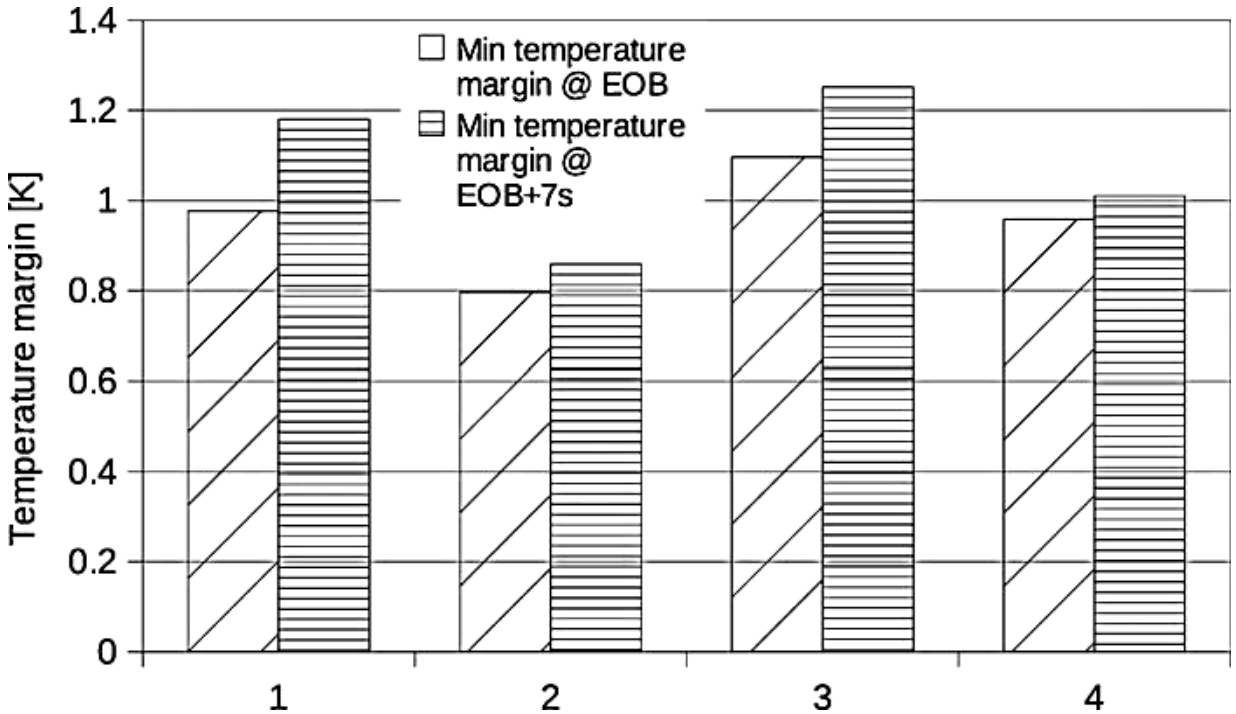

Figure 7. Minimum temperature margins in the four different scenarios at EOB and 7 s later

Conversely, Fig. 8 and Fig. 9 show the temperature margin space distribution at the EOB and its time evolution at the most critical location, in the four different cases considered. Note that nuclear heating was started at 293 s because the residence time of helium in the conductor unit length is 239 s and approximately 270 s were needed to bring the simulation to a stationary state.
Although from Fig. 8 one may be brought to the conclusion that the case cooling and the neutron shield have the same effect in the temperature margin, from Fig. 9 it is apparent that the effect of the shield is lost after the EOB when the heating from steel casing comes to play on the conductor.

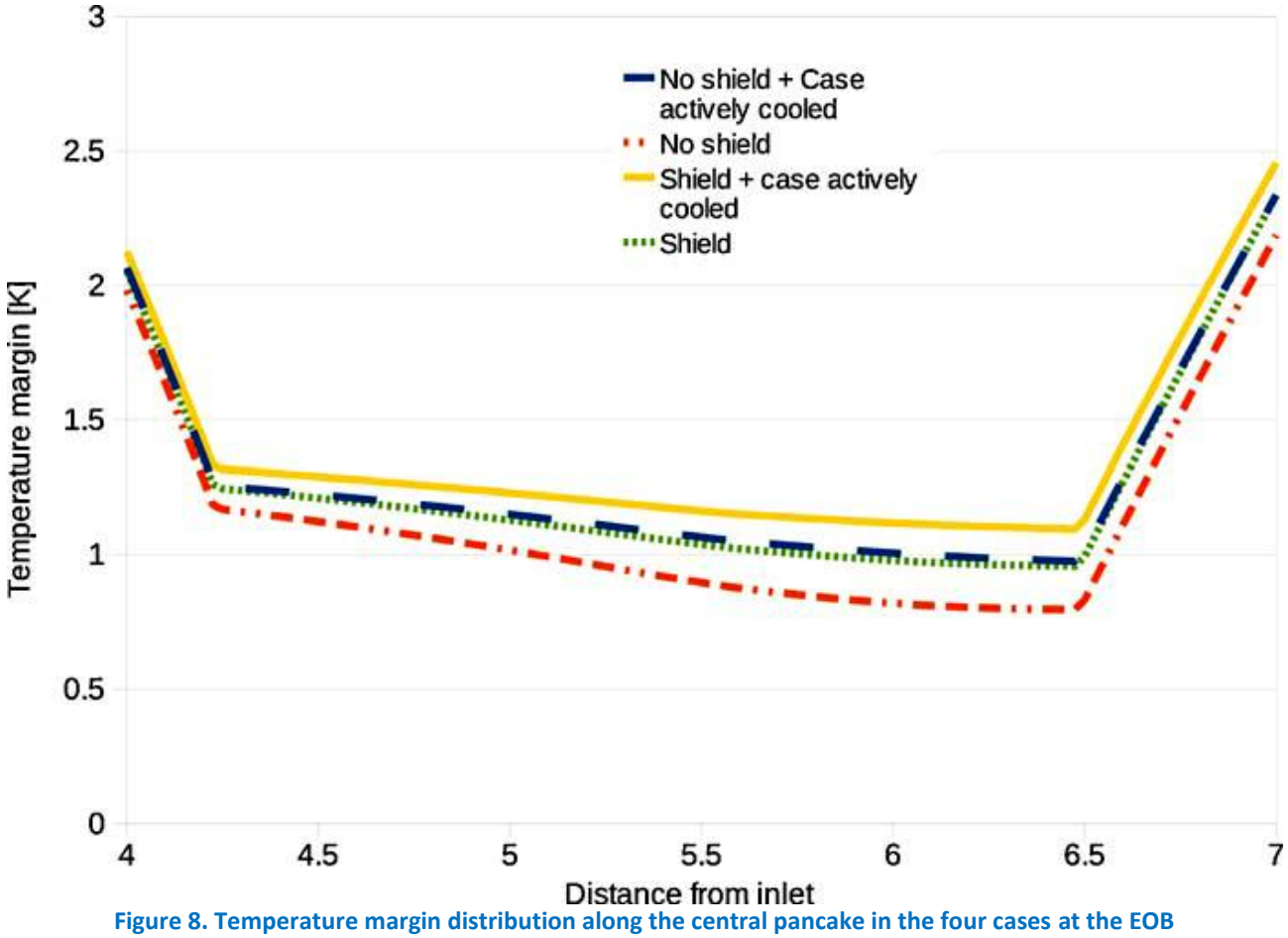

Figure 8. Temperature margin distribution along the central pancake in the four cases at the EOB

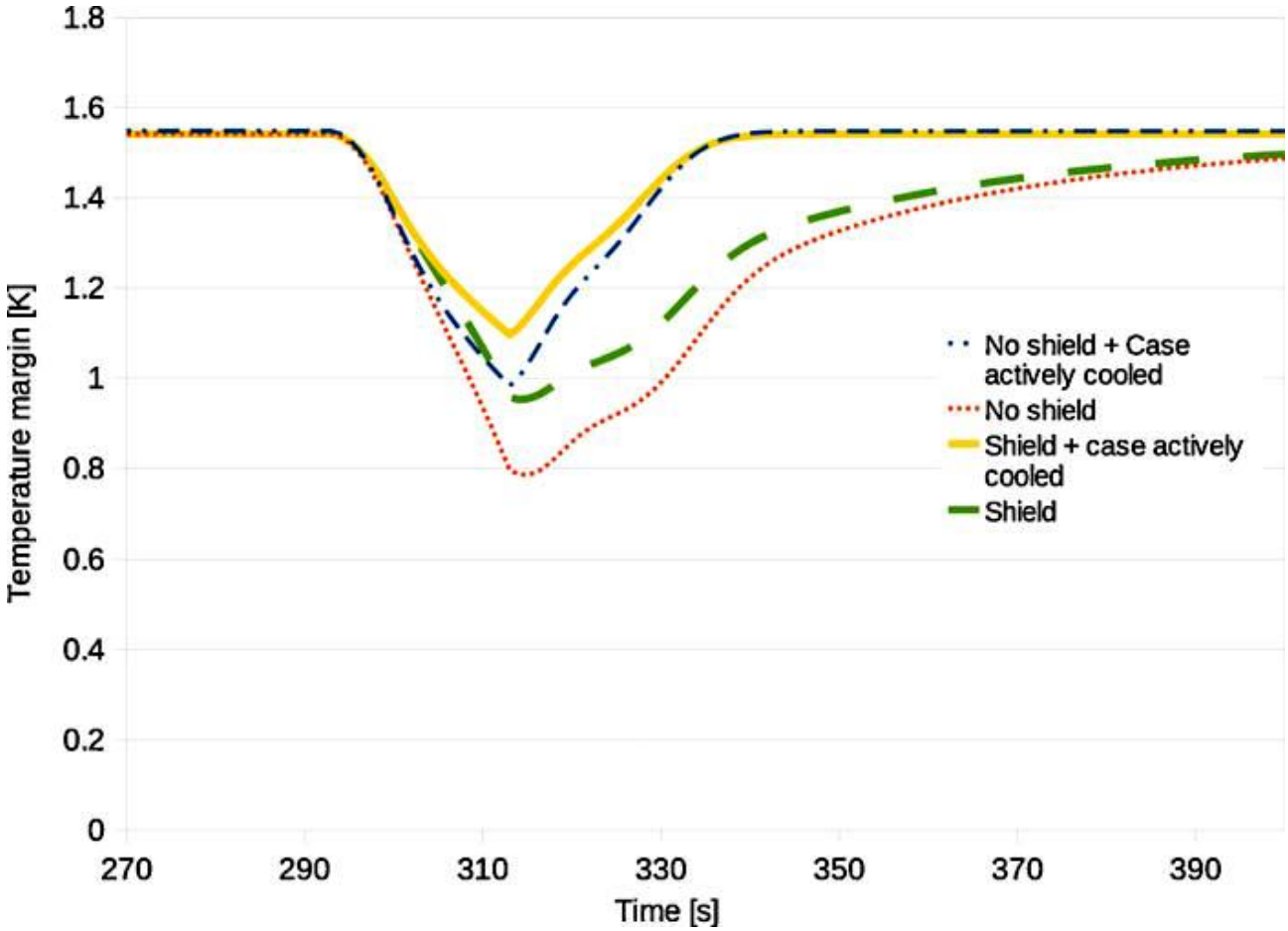

Figure 9. Temperature margin evolution in the most critical location (equatorial plane) in the four cases

3 Conclusion

A preliminary analysis of the temperature margin of the FAST SC TF coil proposal shows that in the given thermal load distribution on winding and coil case due to nuclear heating only, helium inlet to the winding at 4.4 K, and a Mass Flow Rate (MFR) of 4 g/s in the conductor, the computed minimum margin is ~0.9–1.0 K for nominal burn operation. Nonetheless, a refinement of the used models is mandatory before coming to a definite positive conclusion on the present design. Indeed, a more realistic effect of the casing heating to WP and eventually the effect of plasma disruption and AC losses in the conductor should be considered.

4 References

[1] F. Crisanti, A. Cucchiaro, R. Albanese, G. Artaserse, M. Baruzzo, T. Bolzonella, et al., FAST: a European ITER satellite Experiment in the view of DEMO, Fusion Eng. Des., doi:10.1016/j.fusengdes.2011.02.065.

[2] A. Cucchiaro, R. Albanese, G. Ambrosino, G. Brolatti, G. Calabrò, V. Cocilovo, et al., Fusion Eng. Des. 85(2) (2010) 174–180.

[3] G. Ramogida, F. Crisanti, A. Di Zenobio, et al., Studio sulla fattibilità di un sistema magnetico poloidale e toroidale superconduttore per FAST, Report RdS/PAR2014/060, ENEA (2015).

[4] G.M. Polli, L. Reccia, A. Cucchiaro, A. della Corte, A. Di Zenobio, L. Muzzi, et al., Fusion Eng. Des. 84 (2009) 1531–1538.

[5] G. Ramogida, G. Calabro, V. Cocilovo, F. Crisanti, A. Cucchiaro, M. Marinucci, et al., Plasma scenarios, equilibrium configurations and control in the design of FAST, Fusion Eng. Des. 84 (2009) 1562–1569.

[6] R. Villari, A. Cucchiaro, B. Esposito, D. Marocco, F. Moro, L. Petrizzi, et al., Neutronic analysis of FAST, IEEE Trans. Plasma Sci. 38 (March (3)) (2010) 406–413.

[7] R. Bonifetto et al. Computation of JT-60SA TF coil temperature margin, Fusion Eng. Des. 86(6-8) (2011) 1493-1496.
[8] L. Bottura, J. Comp. Phys. 124(1) (1996).
[9] X. Feng Lu, S. Pragnell, D.P. Hampshire, Appl. Phys. Lett. 91 (2007) 132512.

5 Acronyms

SC	Super Conducting
TF	Toroidal Field
PF	Poloidal Field
CS	Central Solenoid
DP	Double Pancake
WP	Winding Pack
VF	Void Fraction
CICC	Cable-In-Conduit-Conductor
NH	Nuclear Heating
SS	Stainless Steel
EOB	End Of Burning
MFR	Mass Flow Rate